IEEE Access
Multidisciplinary ⋮ Rapid Review ⋮ Open Access Journal

Received October 21, 2020, accepted October 29, 2020, date of publication November 3, 2020, date of current version November 13, 2020.

*Digital Object Identifier 10.1109/ACCESS.2020.3035436*

# Reconfigurable Nonlinear Dynamic Inversion for Attitude Control of a Structurally Damaged Aircraft

**QIZHI HE[1], YI TAN[1], XIAOXIONG LIU[1], QIANLEI JIA[1], AND JINGLONG LIU[2]**
[1]Department of Automatic Control, Northwestern Polytechnical University, Xi'an 710072, China
[2]Shanghai Institute of Aerospace System Engineering, Shanghai 201109, China

Corresponding author: Qianlei Jia (jiaql@mail.nwpu.edu.cn)

This work was supported in part by the- National Natural Science Foundation of China under Grant 61573286, Grant 62073266, and Grant 61374032; and in part by the Shaanxi Province Key Laboratory of Flight Control and Simulation Technology.

**ABSTRACT** Structural damage induces extensive parameter changes of an aircraft, which leads to the mismatch problem between the offline model and a flying aircraft. Due to extensive parameter changes, motion of a damaged aircraft is difficultly described with a mathematical model. This article uses disturbances in accelerations and angular accelerations to quantify the effects of extensive parameter changes, and derives a mathematical model for a damaged aircraft. Provided that the flight controller of a damaged aircraft has a fixed structure, the mismatch problem may cause the aircraft unstable. Based on the proposed mathematical model, this article proposed a reconfigurable nonlinear dynamic inversion (RNDI) controller for attitude control of a structurally damaged aircraft, which synthesizes a nonlinear disturbance observer (NDO) with a modified nonlinear dynamic inversion (NDI) controller. The NDO is explored to estimate the disturbances in angular accelerations. Afterwards, the estimations are fed into the modified NDI controller realizes control structure reconfiguration. Conventional NDI control law and model reference adaptive control (MRAC) law are compared, and simulation results demonstrate that the proposed RNDI control law is robust to structural damage and possesses satisfactory control performance.

**INDEX TERMS** Active fault-tolerant control, nonlinear dynamic inversion, nonlinear disturbance observer, reconfigurable controller, attitude control, adaptive control, structurally damaged aircraft.

## I. INTRODUCTION

Modern aircraft design requires that a flight control system not only be equipped for various type of faults but also do not experience performance degradation of nominal systems. In the case of fault-tolerant control (FTC) of an aircraft, active fault-tolerant control (AFTC) and passive fault-tolerant control (PFTC) are two common strategies. PFTC techniques are designed to make the system remains insensitive to presumed faults [1]–[3], [5], [6]. Typically, an AFTC is composed of the following subsystems: a) Fault estimator; b) Controller reconfiguration mechanism, and c) Reconfigurable controller. All three subsystems have to work in harmony within the real time constraints to achieve an effective AFTC system [7]. One of the outstanding superiorities of AFTC schemes is that it does not appear to have performance degradation in the nominal situations, whereas PFTC achieves robustness at the expense of decreased nominal performance [8].

Review article [7], [9] provide an extensive bibliographical review on FTC. Book [10] elaborates background, benchmark, and techniques on FTC of aircrafts. Hallouzi and Verhaegen present a reconfigurable controller based on subspace predictive control, which can not only handle anticipated faults quickly but also unanticipated faults [11]. Joosten *et al.* implement a reconfigurable controller via synthesizing model predictive control and nonlinear dynamic inversion (NDI) techniques, which allows an aircraft able to recover from structural damage [12]. Lombaerts *et al.* investigate an adaptive nonlinear dynamic inversion controller based on online physical model identification to deal with a structurally damaged aircraft control problem [13]. Castaldi and Mimmo develop an AFTC scheme based on a geometric approach in case of actuator and sensor faults [14]. Beyond the above model-based design methods, there is a different design

The associate editor coordinating the review of this manuscript and approving it for publication was Yu Wang.

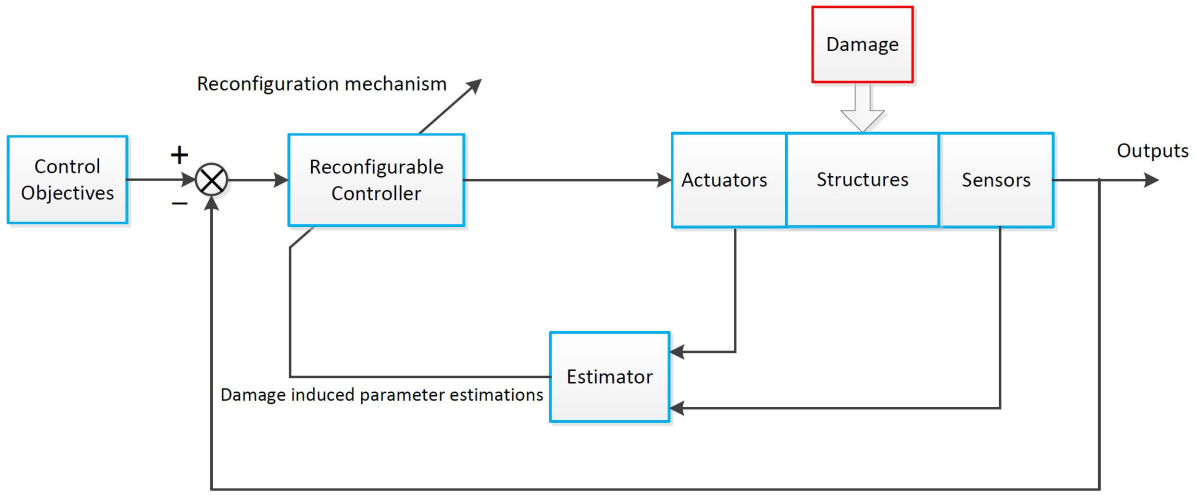


**FIGURE 1.** Framework of a reconfigurable controller subject to structural damage.

philosophy in data-driven monitoring and safety control of industrial cyber-physical systems, which takes advantage of historical input-output data rather than the demanding knowledge about the systems' mechanism models [15]. Reference [16]–[18] utilizes fuzzy adaptive control techniques to realize AFTC when subjected to actuator faults. Kamal *et al.* proposed a fuzzy multi-observer switching control strategy for fault tolerant control of variable-speed wind energy conversion systems in the presence of wide wind variation, wind disturbance, parametric uncertainties, and sensors faults [16]. Shin and Kim present a reconfigurable flight controller which uses online learning neural networks to compensate for a backstepping controller in the presence of control surface damage [19]. Although there are many AFTC methods, it can be classified into two categories. One is designing a bank of controllers offline that switche according to the information provided via estimators. The other is an online reconfigurable controller that incorporates with an estimator. The common philosophy of the two approaches is that the controller is reconfigured according to posterior model information which is recursively updated via synthesizing prior model information and input-output data.

Aircraft faults can be classified into three categories: actuator fault, sensor fault, and structural damage. Among which, structural damage is much more challenging due to the fault-induced extensive changes of aerodynamic coefficients, manipulation coefficients, moments of inertia, mass, and so on [2]. In the case of reconfigurable control for structurally damaged aircrafts, where our research interest resides, research work is found in both dynamics oriented study and a control oriented investigation. Huang and Stengel investigated proportional-integral implicit model-following control for a system with structural damage [20]. Bodson and Groszkiewicz proposed a stabilized recursive least-squares with a forgetting factor algorithm for a damaged aircraft control [21]. Boskovic and Mehra developed an intelligent adaptive reconfigurable control scheme for a tailless advanced fighter aircraft in the presence of wings damage [22]. Lavretsky proposed a composite model reference adaptive control (MRAC) for multi-input multi-output dynamical systems with matched uncertainties [23]. NASA proposed a hybrid direct-indirect neural network adaptive control method and its performance was tested in a medium-fidelity simulation environment with a partial wing loss Generic Transport Model [24]. Patel *et al.* compared the L1 adaptive controller with the conventional model reference adaptive control scheme to show improved transient command tracking and time delay margin [25]. Jourdan presented results from a series of flight tests performed under the DARPA-sponsored damage tolerance control program and four control schemes were discussed and illustrated with actual flight data [26].

Reference [27] proposed a nonlinear disturbance observer (NDO) for fault diagnosis of aircrafts. Based on the proposed NDO scheme, this paper investigates controller reconfigurable mechanisms for a structurally damaged aircraft. Fig.1 shows the framework of a reconfigurable scheme. The estimator is based on a NDO and the reconfigurable controller is based on Nonlinear dynamic inversion (NDI) control. The estimator utilizes the information of actuators and sensors, and generates the damage induced parameter estimations. When there is no damage, the estimator outputs are nearly zeros and the controller runs a nominal control law. When damage occurs, the estimator delivers a new system description and a new set of constraints to the controller. Therefore, the controller is able to maintain overall system stability with acceptable performance in spite of structural damage exists via reconfiguring the nominal control law.

For the attitude control problem of a structurally damaged aircraft, there are three difficulties:

1) Due to structural damage induces extensive parameter changes, the motion of a structurally damaged aircraft is difficultly modeled.

2) Disturbances in angular acceleration cannot directly measured via onboard sensors.
3) States of structurally damaged aircrafts are strongly nonlinear and coupling in a flight envelope. For conventional NDI control laws, controlled states of an aircraft do not contain Euler angles [28], and it has a fixed structure which is sensitive to model uncertainties.

Specific to the above problems, this article:

1) uses disturbances in accelerations and angular accelerations to quantify the extensive parameter changes induced by structural damage. Based on the quantization, a mathematical model of a structurally damaged aircraft is derived.
2) utilizes a NDO to estimate disturbances in angular accelerations via fusing gyroscope and control surface deflection measurements.
3) proposes a reconfigurable nonlinear dynamic inversion (RNDI) control law via synthesizing a NDO with a modified NDI controller, which is able to control Euler angles directly. It decouples states, cancels nonlinearities, compensates model uncertainties, which makes an aircraft not only possess consistent performance without gain scheduling in a flight envelope, but also be robust to structural damage.

## II. PRELIMINARIES

This section elaborates upon knowledge of an improved NDO and NDI control law, which are key techniques applied in the proposed reconfigurable scheme.

### A. NONLINEAR DISTURBANCE OBSERVER

Conventional NDO algorithms require the availability of state derivative measurements, while it is may not always met in real applications. Chen *et al.* proposed an improved NDO for the control of robot manipulators which removes this restriction [29].

Consider a nonlinear system which can be written in:

$$\begin{cases} \dot{x} = f(x) + B(x)u + U(x)\triangle \\ y = Cx \end{cases} \tag{1}$$

where: $x$, $u$, $y$, and $\triangle$ denote system states, control inputs, system outputs, and model uncertainties respectively. And $f(x)$ represents nonlinear terms, $B(x)$ represents the input distribution matrix, $U(x)$ represents uncertainty distribution matrix, and $C$ represents output distribution matrix and it is assumed to be invertible. For the system that can be described as the form of (1), there exists an improved NDO:

$$\begin{cases} \dot{z} = -l(x)U(x)z - l(x)\left[U(x)p(x) + f(x) + B(x)u\right] \\ \hat{\triangle} = z + p(x) \end{cases} \tag{2}$$

where: $\hat{\triangle}$ indicates model uncertainty estimations, $l(x)$ represents observer gain matrix, $z$ is an auxiliary vector, and $p(x)$ is a function vector. Defining model uncertainty estimation errors $e_\triangle$ as:

$$e_\triangle = \hat{\triangle} - \triangle \tag{3}$$

Assuming model uncertainties $\triangle$ are constants:

$$\dot{\triangle} = 0 \tag{4}$$

Differentiating the equation (3) with respect to time and substituting (1), (2), and (4) into it yields the estimation error dynamic equation of the improved NDO:

$$\begin{aligned} \dot{e}_\triangle &= \dot{\hat{\triangle}} - \dot{\triangle} \\ &= (\dot{z} + \frac{\partial p(x)}{\partial x}\dot{x}) - 0 \\ &= -\left[l(x)U(x)(z + p(x)) - \frac{\partial p(x)}{\partial x}U(x)\triangle\right] \\ &\quad + (\frac{\partial p(x)}{\partial x} - l(x))f(x) \\ &\quad + (\frac{\partial p(x)}{\partial x} - l(x))B(x)u \end{aligned} \tag{5}$$

Provided that the observer gain matrix $l(x)$ and the function vector $p(x)$ satisfy the relation:

$$l(x) = \frac{\partial p(x)}{\partial x} \tag{6}$$

Substituting (2), (3), and (6) into (5), the estimation error dynamic equation will reduce to:

$$\dot{e}_\triangle = -l(x)U(x)e_\triangle \tag{7}$$

Which presents that model uncertainty estimation errors are exponentially decayed to zeros in a finite time provided that the designed observer gain matrix $l(x)$ makes the state-transition matrix $-l(x)U(x)$ Hurwitz stable all the time. Therefore, the $i$-th element of the function vector $p(x)$ can be chosen as:

$$p_i(x) = l_{i1}x_1 + l_{i2}x_2 + \ldots + l_{in}x_n \tag{8}$$

where: $x_i$ denotes the $i$-th state, and $l_{ij}$ denotes the element stay at the $i$-th row and $j$-th column of the observer gain matrix $l(x)$. In spite of assuming the model uncertainties are constants, the improved NDO is able to estimate non-constant model uncertainties with exponential decayed estimation errors. Provided that the pole magnitudes assigned to the estimation error dynamics are relatively big enough, the improved NDO still possesses satisfactory performance for the non-constant model uncertainty estimation problem.

### B. NONLINEAR DYNAMIC INVERSION

For the nonlinear system (1), NDI control law is:

$$u = B^{-1}(x)(\dot{x}_{des} - f(x) - U(x)\triangle) \tag{9}$$

where: $\dot{x}_{des}$ denotes the desired close-loop system dynamic. It is usually designed as a first order system:

$$\dot{x}_{des} = K(x_{ref} - x) \tag{10}$$

where: $x_{ref}$ represents reference control objectives, and $K$ denotes gains of controller which are determined according

to the real applications. Feeding the NDI control law (9) into the nonlinear system (1) yields close-loop dynamics:

$$\begin{cases} \dot{x} = \dot{x}_{des} = K(x_{ref} - x) \\ y = Cx \end{cases} \tag{11}$$

Implementing Laplace transformation to the close-loop system (11) yields:

$$y(s) = C(sI + K)^{-1} K x_{ref}(s) \tag{12}$$

Which means that the close-loop dynamics are first order systems with time constants:

$$T = K^{-1} \tag{13}$$

Defining the control errors as:

$$e_x = x_{ref} - x \tag{14}$$

Assuming the reference control objectives are constants:

$$\dot{x}_{ref} = 0 \tag{15}$$

Differentiating the equation (14) with respect to time and substituting (11) and (15) into it yields the control error dynamics:

$$\dot{e}_x = \dot{x}_{ref} - \dot{x} = -\dot{x} = -Ke_x \tag{16}$$

Therefore, control errors are exponentially decayed to zeros in a finite time provided that the gains of NDI control law are chosen as positive scales.

## III. RECONFIGURABLE CONTROLLER

This section elaborates on modeling and controller reconfiguration mechanisms for a structurally damaged aircrafts via synthesizing improved NDO and NDI techniques.

### A. STRUCTURALLY DAMAGED AIRCRAFT MODELING

Moment equations and force equations are dynamic equations of aircrafts that are influenced by structural damage. While attitude equations and position equations are kinematic equations, they are not influenced by structural damage. Structural damage induces extensive parameter changes in an inertial matrix, aerodynamic coefficients, and so on. It is impossible to consider all the parameters accurately. This subsection utilizes additive disturbances in accelerations and angular accelerations to quantify the structural damage induced model uncertainties in dynamic equations.

#### 1) MOMENT EQUATIONS

$$\begin{bmatrix} \dot{p} \\ \dot{q} \\ \dot{r} \end{bmatrix} = I_b^{-1} \left( \begin{bmatrix} L \\ M \\ N \end{bmatrix} - \begin{bmatrix} p \\ q \\ r \end{bmatrix} \times I_b \begin{bmatrix} p \\ q \\ r \end{bmatrix} \right) + \begin{bmatrix} \triangle_{\dot{p}} \\ \triangle_{\dot{q}} \\ \triangle_{\dot{r}} \end{bmatrix} \tag{17}$$

where: $p$, $q$, and $r$ are rotational rates represented in body frame, which are measured via gyroscopes. $L$, $M$, and $N$ are moments represented in body frame. $\triangle_{\dot{p}}$, $\triangle_{\dot{q}}$, and $\triangle_{\dot{r}}$ represent disturbances in angular accelerations, namely the quantified model uncertainties induced by structural damage. $I_b$ is the inertia matrix defined as:

$$I_b = \begin{bmatrix} I_{xx} & -I_{xy} & -I_{xz} \\ -I_{xy} & I_{yy} & -I_{yz} \\ -I_{xz} & -I_{yz} & I_{zz} \end{bmatrix} \tag{18}$$

#### 2) ATTITUDE EQUATIONS

$$\begin{bmatrix} \dot{\phi} \\ \dot{\theta} \\ \dot{\psi} \end{bmatrix} = \begin{bmatrix} 1 & \tan\theta \sin\phi & \tan\theta \cos\phi \\ 0 & \cos\phi & -\sin\phi \\ 0 & \sin\phi / \cos\theta & \cos\phi / \cos\theta \end{bmatrix} \begin{bmatrix} p \\ q \\ r \end{bmatrix} \tag{19}$$

where: $\phi$, $\theta$, and $\psi$ represent Euler angles.

#### 3) FORCE EQUATIONS

$$\begin{bmatrix} \dot{u} \\ \dot{v} \\ \dot{w} \end{bmatrix} = \begin{bmatrix} -g\sin\theta \\ g\sin\phi\cos\theta \\ g\cos\phi\cos\theta \end{bmatrix} - \begin{bmatrix} qw - rv \\ ru - pw \\ pv - qu \end{bmatrix} + \frac{1}{m + \triangle_m} \begin{bmatrix} \bar{X} + \triangle_{\bar{X}} \\ \bar{Y} + \triangle_{\bar{Y}} \\ \bar{Z} + \triangle_{\bar{Z}} \end{bmatrix} \tag{20}$$

Structural damage induced model uncertainties in force equations can be quantified by acceleration changes, and accelerations can be directly measured. Therefore, force equations can be represented as a simplified form:

$$\begin{bmatrix} \dot{u} \\ \dot{v} \\ \dot{w} \end{bmatrix} = \begin{bmatrix} -g\sin\theta \\ g\sin\phi\cos\theta \\ g\cos\phi\cos\theta \end{bmatrix} - \begin{bmatrix} qw - rv \\ ru - pw \\ pv - qu \end{bmatrix} + \begin{bmatrix} A_x \\ A_y \\ A_z \end{bmatrix} \tag{21}$$

where: $m$ denotes mass of an aircraft. $g$ denotes gravity acceleration. $u$, $v$, and $w$ are velocities represented in body frame. $A_x$, $A_y$, and $A_z$ are accelerations represented in body frame. $\bar{X}$, $\bar{Y}$, and $\bar{Z}$ are total forces represented in body frame. $\triangle_m$, $\triangle_{\bar{X}}$, $\triangle_{\bar{Y}}$, and $\triangle_{\bar{Z}}$ represents the quantified model uncertainties in mass and forces.

#### 4) POSITION EQUATIONS

$$\begin{bmatrix} \dot{x} \\ \dot{y} \\ \dot{z} \end{bmatrix} = T_b^e \begin{bmatrix} u \\ v \\ w \end{bmatrix} \tag{22}$$

where: $x$, $y$, and $z$ represent positions in earth frame. $T_b^n$ denotes the coordinate transform matrix from body frame to earth frame.

$$T_b^e = \begin{bmatrix} c\theta c\psi & s\phi s\theta c\psi - c\phi s\psi & c\phi s\theta c\psi + s\phi s\psi \\ c\theta s\psi & s\phi s\theta s\psi + cs\phi c\psi & c\phi s\theta s\psi - s\phi c\psi \\ -s\theta & s\phi c\theta & c\phi c\theta \end{bmatrix} \tag{23}$$

For simplicity, $s(\bullet)$, $c(\bullet)$ and $t(\bullet)$ denote $sin(\bullet)$, $cos(\bullet)$ and $tan(\bullet)$ respectively.

### B. RECONFIGURATION MECHANISM

Equations (17), (19), (21) and (22) make up a structurally damaged aircraft motion model, among which $L$, $M$, $N$, and $I_b$ are calculated from wind tunnel test data. When structural damage occurs, the offline model generated from wind tunnel

test data mismatches a real system. Therefore, $\triangle_{\dot{p}}$, $\triangle_{\dot{q}}$, and $\triangle_{\dot{r}}$ are explored to compensate the errors between an offline model and a real system. Whereas, $\triangle_{\dot{p}}$, $\triangle_{\dot{q}}$, and $\triangle_{\dot{r}}$ are unknown, it required to be estimated online according to control inputs $u$ and sensor measurements $y$. Provided that there are accurate estimations of $\hat{\triangle}_{\dot{p}}$, $\hat{\triangle}_{\dot{q}}$, and $\hat{\triangle}_{\dot{r}}$, the errors between an offline model and a real system can be well compensated.

#### 1) ESTIMATOR

For a structurally damaged aircraft, improved NDO is explored to estimate $\triangle_{\dot{p}}$, $\triangle_{\dot{q}}$, and $\triangle_{\dot{r}}$. For moments:

$$\begin{bmatrix} L \\ M \\ N \end{bmatrix} = \bar{q}S \begin{bmatrix} b & 0 & 0 \\ 0 & \bar{c} & 0 \\ 0 & 0 & b \end{bmatrix} \begin{bmatrix} C_L \\ C_M \\ C_N \end{bmatrix} \tag{24}$$

where: $\bar{q}$ denotes dynamic pressure, $S$ denotes wing surface area, $b$ denotes wing span, and $\bar{c}$ denotes mean aerodynamic chord. $C_L$, $C_M$, and $C_N$ are rolling moment coefficient, pitching moment coefficient, and yawing moment coefficient respectively. The moment coefficients are online calculated according to current states, control surface deflections, aero data and so on, which can be represented as:

$$\begin{bmatrix} C_L \\ C_M \\ C_N \end{bmatrix} = \begin{bmatrix} C_{\bar{L}} \\ C_{\bar{M}} \\ C_{\bar{N}} \end{bmatrix} + \begin{bmatrix} C_{L\delta_a} & 0 & C_{L\delta_r} \\ 0 & C_{M\delta_e} & \\ C_{N\delta_a} & 0 & C_{N\delta_r} \end{bmatrix} \begin{bmatrix} \delta_a \\ \delta_e \\ \delta_r \end{bmatrix} \tag{25}$$

where: $C_{\bar{L}}$, $C_{\bar{M}}$, and $C_{\bar{N}}$ represent all the terms except manipulation related terms. Therefore the second term of equation (25) denotes the manipulation related terms, among which $C_{L\delta_a}$, $C_{L\delta_r}$, $C_{M\delta_e}$, $C_{N\delta_a}$, and $C_{N\delta_r}$ are manipulation coefficients. $\delta_a$, $\delta_e$, and $\delta_r$ denote the deflections of aileron, elevator, and rudder respectively. Substituting (24) and (25) into (17) yields:

$$\begin{aligned} \begin{bmatrix} \dot{p} \\ \dot{q} \\ \dot{r} \end{bmatrix} &= I_b^{-1}(\bar{q}S \begin{bmatrix} b & 0 & 0 \\ 0 & \bar{c} & 0 \\ 0 & 0 & b \end{bmatrix} \begin{bmatrix} C_{\bar{L}} \\ C_{\bar{M}} \\ C_{\bar{N}} \end{bmatrix} - \begin{bmatrix} p \\ q \\ r \end{bmatrix} \times I_b \begin{bmatrix} p \\ q \\ r \end{bmatrix}) \\ &\quad + I_b^{-1}\bar{q}S \begin{bmatrix} b & 0 & 0 \\ 0 & \bar{c} & 0 \\ 0 & 0 & b \end{bmatrix} \begin{bmatrix} C_{L\delta_a} & 0 & C_{L\delta_r} \\ 0 & C_{M\delta_e} & \\ C_{N\delta_a} & 0 & C_{N\delta_r} \end{bmatrix} \begin{bmatrix} \delta_a \\ \delta_e \\ \delta_r \end{bmatrix} \\ &\quad + \begin{bmatrix} \triangle_{\dot{p}} \\ \triangle_{\dot{q}} \\ \triangle_{\dot{r}} \end{bmatrix} \end{aligned} \tag{26}$$

Selecting rotational rates as system states, and it can be measured by gyroscopes:

$$x = \begin{bmatrix} p \\ q \\ r \end{bmatrix} \approx \begin{bmatrix} p_m \\ q_m \\ r_m \end{bmatrix} \tag{27}$$

where: $p_m$, $q_m$, and $r_m$ represent gyroscope measurements. Control surface deflections are control inputs, and it is can be measured by angle sensors:

$$u = \begin{bmatrix} \delta_a \\ \delta_e \\ \delta_r \end{bmatrix} \approx \begin{bmatrix} \delta_{am} \\ \delta_{em} \\ \delta_{rm} \end{bmatrix} \tag{28}$$

where: $\delta_{am}$, $\delta_{em}$, and $\delta_{rm}$ represent deflection angle measurements of aileron, elevator, and rudder respectively. Comparing equations (26) with (1) yields:

$$f(x) = I_b^{-1}(\bar{q}S \begin{bmatrix} b & 0 & 0 \\ 0 & \bar{c} & 0 \\ 0 & 0 & b \end{bmatrix} \begin{bmatrix} C_{\bar{L}} \\ C_{\bar{M}} \\ C_{\bar{N}} \end{bmatrix} - \begin{bmatrix} p \\ q \\ r \end{bmatrix} \times I_b \begin{bmatrix} p \\ q \\ r \end{bmatrix}) \tag{29}$$

$$B(x) = I_b^{-1}\bar{q}S \begin{bmatrix} b & 0 & 0 \\ 0 & \bar{c} & 0 \\ 0 & 0 & b \end{bmatrix} \begin{bmatrix} C_{L\delta_a} & 0 & C_{L\delta_r} \\ 0 & C_{M\delta_e} & \\ C_{N\delta_a} & 0 & C_{N\delta_r} \end{bmatrix} \tag{30}$$

$$U(x) = \begin{bmatrix} 1 & 0 & 0 \\ 0 & 1 & 0 \\ 0 & 0 & 1 \end{bmatrix} \tag{31}$$

$$\triangle = \begin{bmatrix} \triangle_{\dot{p}} \\ \triangle_{\dot{q}} \\ \triangle_{\dot{r}} \end{bmatrix} \tag{32}$$

Due to $U(x)$ is a identity matrix, in order to make the state-transition matrix $-l(x)U(x)$ Hurwitz stable, the observer gain matrix are designed as:

$$l(x) = \begin{bmatrix} 10 & 0 & 0 \\ 0 & 10 & 0 \\ 0 & 0 & 10 \end{bmatrix} \tag{33}$$

Substituting (27) and (33) into equation (8) yields:

$$p(x) = \begin{bmatrix} 10 \cdot p_m \\ 10 \cdot q_m \\ 10 \cdot r_m \end{bmatrix} \tag{34}$$

Substituting (27) - (34) into NDO (2) yields the estimations of quantified structural damage induced model uncertainties $\hat{\triangle}_{\dot{p}}$, $\hat{\triangle}_{\dot{q}}$, and $\hat{\triangle}_{\dot{r}}$:

$$\begin{cases} \begin{bmatrix} \dot{z}_1 \\ \dot{z}_2 \\ \dot{z}_3 \end{bmatrix} = -\begin{bmatrix} 10 & 0 & 0 \\ 0 & 10 & 0 \\ 0 & 0 & 10 \end{bmatrix} \begin{bmatrix} z_1 \\ z_2 \\ z_3 \end{bmatrix} \\ \qquad - \begin{bmatrix} 10 & 0 & 0 \\ 0 & 10 & 0 \\ 0 & 0 & 10 \end{bmatrix} \{ \begin{bmatrix} 10 \cdot p_m \\ 10 \cdot q_m \\ 10 \cdot r_m \end{bmatrix} \\ + I_b^{-1}(\bar{q}S \begin{bmatrix} b & 0 & 0 \\ 0 & \bar{c} & 0 \\ 0 & 0 & b \end{bmatrix} \begin{bmatrix} C_{\bar{L}} \\ C_{\bar{M}} \\ C_{\bar{N}} \end{bmatrix} - \begin{bmatrix} p_m \\ q_m \\ r_m \end{bmatrix} \times I_b \begin{bmatrix} p_m \\ q_m \\ r_m \end{bmatrix}) \\ + I_b^{-1}\bar{q}S \begin{bmatrix} b & 0 & 0 \\ 0 & \bar{c} & 0 \\ 0 & 0 & b \end{bmatrix} \begin{bmatrix} C_{L\delta_a} & 0 & C_{L\delta_r} \\ 0 & C_{M\delta_e} & \\ C_{N\delta_a} & 0 & C_{N\delta_r} \end{bmatrix} \begin{bmatrix} \delta_{am} \\ \delta_{em} \\ \delta_{rm} \end{bmatrix} \} \\ \begin{bmatrix} \hat{\triangle}_{\dot{p}} \\ \hat{\triangle}_{\dot{q}} \\ \hat{\triangle}_{\dot{r}} \end{bmatrix} = \begin{bmatrix} z_1 \\ z_2 \\ z_3 \end{bmatrix} + \begin{bmatrix} 10 \cdot p_m \\ 10 \cdot q_m \\ 10 \cdot r_m \end{bmatrix} \end{cases} \tag{35}$$

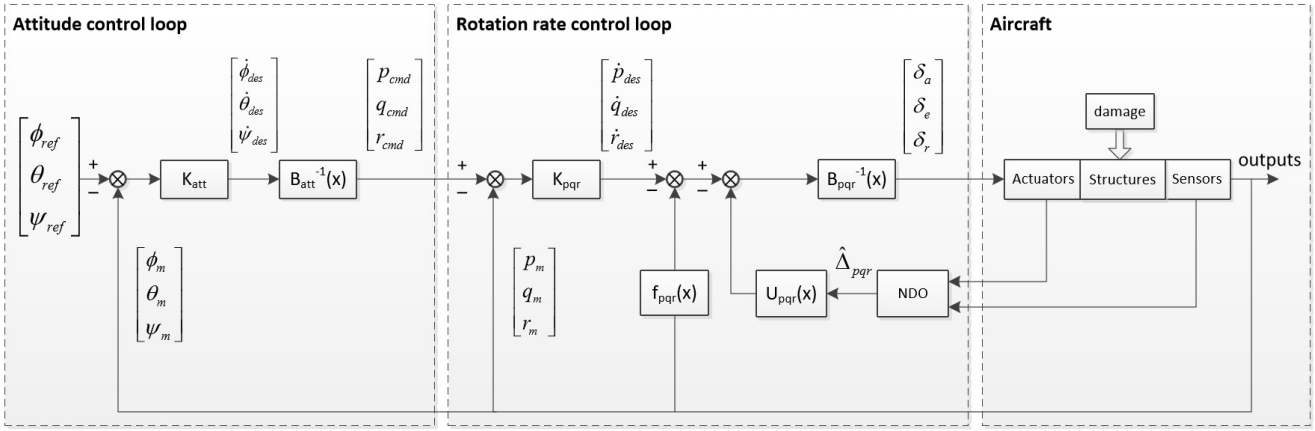


**FIGURE 2.** Architecture of reconfigurable nonlinear dynamic inversion for the attitude control of a structural damaged aircraft.

*Remarks:* For the conventional MRAC control method, $\hat{\Delta}_{\dot{p}}$, $\hat{\Delta}_{\dot{q}}$, and $\hat{\Delta}_{\dot{r}}$ are calculated according to transformation of equation (26):

$$\begin{aligned}\begin{bmatrix}\hat{\Delta}_{\dot{p}}\\ \hat{\Delta}_{\dot{q}}\\ \hat{\Delta}_{\dot{r}}\end{bmatrix} &= -I_b^{-1}(\bar{q}S\begin{bmatrix}b&0&0\\0&\bar{c}&0\\0&0&b\end{bmatrix}\begin{bmatrix}C_{\bar{L}}\\C_{\bar{M}}\\C_{\bar{N}}\end{bmatrix}-\begin{bmatrix}p_m\\q_m\\r_m\end{bmatrix}\times I_b\begin{bmatrix}p_m\\q_m\\r_m\end{bmatrix})\\ &\quad -I_b^{-1}\bar{q}S\begin{bmatrix}b&0&0\\0&\bar{c}&0\\0&0&b\end{bmatrix}\begin{bmatrix}C_{L\delta_a}&0&C_{L\delta_r}\\0&C_{M\delta_e}&\\C_{N\delta_a}&0&C_{N\delta_r}\end{bmatrix}\begin{bmatrix}\delta_{am}\\\delta_{em}\\\delta_{rm}\end{bmatrix}\\ &\quad +\begin{bmatrix}\dot{p}_m\\\dot{q}_m\\\dot{r}_m\end{bmatrix}\end{aligned} \tag{36}$$

where: $\dot{p}_m$, $\dot{q}_m$, and $\dot{r}_m$ are acquired via differentiating the gyroscope measurements with respect to sample time.

### 2) RECONFIGURABLE ATTITUDE CONTROLLER

Fig.2 shows the architecture of the RNDI control law for the attitude control problem of a structurally damaged aircraft. It can be divided as two control loops, an attitude control loop and a rotation rate control loop. According to equation (13), the close-loop dynamics are first order systems with time constants equal to $K^{-1}$. Provided that the controller gains $K$ for a rotation rate control loop are much bigger than an attitude control loop, the multi-states system control problem can be decoupled into two cascaded reduced order subsystem control problems.

For an attitude control loop, the state vector are Euler angles which can be measured by a navigation system.

$$x_{att} = \begin{bmatrix}\phi\\\theta\\\psi\end{bmatrix} \approx \begin{bmatrix}\phi_m\\\theta_m\\\psi_m\end{bmatrix} \tag{37}$$

where: $\phi_m$, $\theta_m$, and $\psi_m$ represent attitude measurements. The inputs are the attitude reference signals:

$$I_{att} = \begin{bmatrix}\phi_{ref}\\\theta_{ref}\\\psi_{ref}\end{bmatrix} \tag{38}$$

where: $\phi_{ref}$, $\theta_{ref}$, and $\psi_{ref}$ represent reference control objectives. The outputs are rotation rate commands, and it is also the virtual control inputs of the rotation rate control loop.

$$O_{att} = u_{vir} = \begin{bmatrix}p_{cmd}\\q_{cmd}\\r_{cmd}\end{bmatrix} \tag{39}$$

where: $p_{cmd}$, $q_{cmd}$, and $r_{cmd}$ represent roll rate, pitch rate, and yaw rate commands respectively. The desired dynamics of an attitude control loop are:

$$\dot{x}_{des}^{att} = \begin{bmatrix}\dot{\phi}_{des}\\\dot{\theta}_{des}\\\dot{\psi}_{des}\end{bmatrix} \tag{40}$$

Desired dynamics are designed according to equation (10):

$$\dot{x}_{des}^{att} = K_{att}(I_{att} - x_{att}) \tag{41}$$

where: $K_{att}$ denotes the gain matrix for attitude control loop. In this paper, gain matrix is designed as:

$$K_{att} = \begin{bmatrix}2&0&0\\0&2&0\\0&0&2\end{bmatrix} \tag{42}$$

Comparing equation (19) with (1) yields:

$$f_{att}(x) = 0 \tag{43}$$

$$B_{att}(x) = \begin{bmatrix}1&\tan\theta\sin\phi&\tan\theta\cos\phi\\0&\cos\phi&-\sin\phi\\0&\sin\phi/\cos\theta&\cos\phi/\cos\theta\end{bmatrix} \tag{44}$$

$$U_{att}(x)\Delta_{att} = 0 \tag{45}$$

Substituting (37) - (45) into equation (9) yields control law for the attitude control loop:

$$\begin{bmatrix} p_{cmd} \\ q_{cmd} \\ r_{cmd} \end{bmatrix} = \begin{bmatrix} 1 & \tan\theta_m \sin\phi_m & \tan\theta_m \cos\phi_m \\ 0 & \cos\phi_m & -\sin\phi_m \\ 0 & \sin\phi_m/\cos\theta_m & \cos\phi_m/\cos\theta_m \end{bmatrix}^{-1} \begin{bmatrix} 2 & 0 & 0 \\ 0 & 2 & 0 \\ 0 & 0 & 2 \end{bmatrix} \begin{bmatrix} \phi_{ref} - \phi_m \\ \theta_{ref} - \theta_m \\ \psi_{ref} - \psi_m \end{bmatrix} \tag{46}$$

For a rotation rate control loop, the state vector is rotation rates which can be measured by gyroscopes.

$$x_{pqr} = \begin{bmatrix} p \\ q \\ r \end{bmatrix} \approx \begin{bmatrix} p_m \\ q_m \\ r_m \end{bmatrix} \tag{47}$$

The inputs of the rotation rate control loop are the outputs of the attitude control loop:

$$I_{pqr} = O_{att} = u_{vir} = \begin{bmatrix} p_{cmd} \\ q_{cmd} \\ r_{cmd} \end{bmatrix} \tag{48}$$

The outputs are control surface deflection angles, and it is also the control inputs of the aircraft.

$$O_{pqr} = u_{pqr} = \begin{bmatrix} \delta_a \\ \delta_e \\ \delta_r \end{bmatrix} \tag{49}$$

The desired dynamics of the rotation rate control loop are:

$$\dot{x}_{des}^{pqr} = \begin{bmatrix} \dot{p}_{des} \\ \dot{q}_{des} \\ \dot{r}_{des} \end{bmatrix} \tag{50}$$

Desired dynamics are designed according to equation (10):

$$\dot{x}_{des}^{pqr} = K_{pqr}(I_{pqr} - x_{pqr}) \tag{51}$$

where: $K_{pqr}$ denotes the gain matrix for the rotation rate control loop. In order to achieve control objectives, the desired dynamics of a rotation rate control loop are required to be faster than an attitude control loop. Therefore, the gains of a rotation rate control loop are required to be bigger, and the gain matrix of the rotation rate control loop is designed as:

$$K_{pqr} = \begin{bmatrix} 10 & 0 & 0 \\ 0 & 10 & 0 \\ 0 & 0 & 10 \end{bmatrix} \tag{52}$$

Comparing equations (26) with (1) yields:

$$f_{pqr}(x) = I_b^{-1}(\bar{q}S \begin{bmatrix} b & 0 & 0 \\ 0 & \bar{c} & 0 \\ 0 & 0 & b \end{bmatrix} \begin{bmatrix} C_{\bar{L}} \\ C_{\bar{M}} \\ C_{\bar{N}} \end{bmatrix} - \begin{bmatrix} p \\ q \\ r \end{bmatrix} \times I_b \begin{bmatrix} p \\ q \\ r \end{bmatrix}) \tag{53}$$

$$B_{pqr} = I_b^{-1}\bar{q}S \begin{bmatrix} b & 0 & 0 \\ 0 & \bar{c} & 0 \\ 0 & 0 & b \end{bmatrix} \begin{bmatrix} C_{L\delta_a} & 0 & C_{L\delta_r} \\ 0 & C_{M\delta_e} & \\ C_{N\delta_a} & 0 & C_{N\delta_r} \end{bmatrix} \tag{54}$$

$$U_{pqr}(x) = \begin{bmatrix} 1 & 0 & 0 \\ 0 & 1 & 0 \\ 0 & 0 & 1 \end{bmatrix} \tag{55}$$

Quantified uncertainties are defined as:

$$\triangle_{pqr} = \begin{bmatrix} \triangle_{\dot{p}} \\ \triangle_{\dot{q}} \\ \triangle_{\dot{r}} \end{bmatrix} \tag{56}$$

The quantified uncertainties are unknown, while it can be estimated via an improved NDO, which is presented in (35).

$$\hat{\triangle}_{pqr} = \begin{bmatrix} \hat{\triangle}_{\dot{p}} \\ \hat{\triangle}_{\dot{q}} \\ \hat{\triangle}_{\dot{r}} \end{bmatrix} \tag{57}$$

Substituting (47) - (57) into equation (9) yields control law:

$$\begin{bmatrix} \delta_a \\ \delta_e \\ \delta_r \end{bmatrix} = (I_b^{-1}\bar{q}S \begin{bmatrix} b & 0 & 0 \\ 0 & \bar{c} & 0 \\ 0 & 0 & b \end{bmatrix} \begin{bmatrix} C_{L\delta_a} & 0 & C_{L\delta_r} \\ 0 & C_{M\delta_e} & \\ C_{N\delta_a} & 0 & C_{N\delta_r} \end{bmatrix})^{-1} \{ \begin{bmatrix} 10 & 0 & 0 \\ 0 & 10 & 0 \\ 0 & 0 & 10 \end{bmatrix} \begin{bmatrix} p_{cmd} - p_m \\ q_{cmd} - q_m \\ r_{cmd} - r_m \end{bmatrix} - I_b^{-1}(\bar{q}S \begin{bmatrix} b & 0 & 0 \\ 0 & \bar{c} & 0 \\ 0 & 0 & b \end{bmatrix} \begin{bmatrix} C_{\bar{L}} \\ C_{\bar{M}} \\ C_{\bar{N}} \end{bmatrix} - \begin{bmatrix} p_m \\ q_m \\ r_m \end{bmatrix} \times I_b \begin{bmatrix} p_m \\ q_m \\ r_m \end{bmatrix}) - \begin{bmatrix} \hat{\triangle}_{\dot{p}} \\ \hat{\triangle}_{\dot{q}} \\ \hat{\triangle}_{\dot{r}} \end{bmatrix} \} \tag{58}$$

*Remarks:* For the NDI control method, controller structures are not changed in spite of structural damage occurs. Therefore, NDI control law is:

$$\begin{bmatrix} \delta_a \\ \delta_e \\ \delta_r \end{bmatrix} = (I_b^{-1}\bar{q}S \begin{bmatrix} b & 0 & 0 \\ 0 & \bar{c} & 0 \\ 0 & 0 & b \end{bmatrix} \begin{bmatrix} C_{L\delta_a} & 0 & C_{L\delta_r} \\ 0 & C_{M\delta_e} & \\ C_{N\delta_a} & 0 & C_{N\delta_r} \end{bmatrix})^{-1} \{ \begin{bmatrix} 10 & 0 & 0 \\ 0 & 10 & 0 \\ 0 & 0 & 10 \end{bmatrix} \begin{bmatrix} p_{cmd} - p_m \\ q_{cmd} - q_m \\ r_{cmd} - r_m \end{bmatrix} - I_b^{-1}(\bar{q}S \begin{bmatrix} b & 0 & 0 \\ 0 & \bar{c} & 0 \\ 0 & 0 & b \end{bmatrix} \begin{bmatrix} C_{\bar{L}} \\ C_{\bar{M}} \\ C_{\bar{N}} \end{bmatrix} - \begin{bmatrix} p_m \\ q_m \\ r_m \end{bmatrix} \times I_b \begin{bmatrix} p_m \\ q_m \\ r_m \end{bmatrix}) \} \tag{59}$$

### C. STABILITY ANALYSIS

The reconfigurable flight control system is composed of a reconfigurable attitude controller and an estimator. Augmenting the estimation errors to the control errors yields the

**TABLE 1. Control laws.**

| Control law | Equations |
|---|---|
| NDI | (46), (59) |
| MRAC | (36), (46), (58) |
| RNDI | (35), (46), (58) |

reconfigurable flight control system errors:

$$e_{sys}(x,\triangle)=\begin{bmatrix}e_x\\e_\triangle\end{bmatrix}=\begin{bmatrix}\phi_{ref}-\phi\\\theta_{ref}-\theta\\\psi_{ref}-\psi\\p_{cmd}-p\\q_{cmd}-q\\r_{cmd}-r\\\hat{\triangle}_{\dot{p}}-\triangle_{\dot{p}}\\\hat{\triangle}_{\dot{q}}-\triangle_{\dot{q}}\\\hat{\triangle}_{\dot{r}}-\triangle_{\dot{r}}\end{bmatrix} \tag{60}$$

Differentiating (60) with respect to time. Afterwards, substituting (7) and (16) into it yields:

$$\dot{e}_{sys}(x,\triangle)=-\begin{bmatrix}K_{att}&0&0\\0&K_{pqr}&0\\0&0&l(x)U(x)\end{bmatrix}e_{sys}(x,\triangle) \tag{61}$$

Selecting a Lyapunov candidate function for the reconfigurable flight control system as:

$$V(x,\triangle)=\frac{1}{2}\cdot e_{sys}^T(x,\triangle)e_{sys}(x,\triangle) \tag{62}$$

Differentiating (62) with respect to time, and substituting (61) into it yields:

$$\begin{aligned}\dot{V}(x,\triangle)&=e_{sys}^T(x,\triangle)\dot{e}_{sys}(x,\triangle)\\&=-e_{sys}^T(x,\triangle)\begin{bmatrix}K_{att}&0&0\\0&K_{pqr}&0\\0&0&l(x)U(x)\end{bmatrix}e_{sys}(x,\triangle)\end{aligned} \tag{63}$$

$V(x,\triangle)$ is positive defined and $\dot{V}(x,\triangle)$ is negative defined. According to the Lyapunov theorem, the control system is asymptotically stable.

*Remarks:* Big controller gains and drastic damage contribute to big control surface deflections which result in control surfaces easily to be saturated. Control surface saturation leads the control performance to degrade significantly, and it may cause an aircraft be unstable. Namely, provided that the control surface saturation does not occur, the proposed RNDI control law is robust to structural damage.

## IV. SIMULATION AND ANALYSIS

This section compares the proposed RNDI control method with conventional NDI and MRAC control approaches via a digital simulation. The corresponding equations of NDI, MRAC, and RNDI control laws are presented in Table 1.

F-16 aircraft model is utilized and it is trimmed as level flight with a velocity at 150 $m/s$ and a height at 1000 $m$. The trimmed states are shown in Table 2, and the trimmed inputs are shown in Table 3. Firstly, open-loop responses, a rotation control loop and an attitude control loop are simulated with given quantified model uncertainties. Afterwards, a structurally damaged F-16 aircraft with extensive parameter changes are simulated to demonstrate the effectiveness of the proposed RNDI control method. Finally, these simulation results are analyzed.

**TABLE 2. Trimmed states.**

| State | Value | Unit |
|---|---|---|
| $u$ | 149.6281 | $m/s$ |
| $v$ | 0 | $m/s$ |
| $w$ | 10.5562 | $m/s$ |
| $p$ | 0 | $deg/s$ |
| $q$ | 0 | $deg/s$ |
| $r$ | 0 | $deg/s$ |
| $\phi$ | 0 | $deg$ |
| $\theta$ | 4.0355 | $deg$ |
| $\psi$ | 0 | $deg$ |
| $h$ | 1000 | $m$ |

**TABLE 3. Trimmed inputs.**

| Input | Value | Unit |
|---|---|---|
| $\delta_e$ | -0.9967 | $deg$ |
| $\delta_a$ | 0 | $deg$ |
| $\delta_r$ | 0 | $deg$ |
| $\delta_t$ | 0.10562 | – |

**TABLE 4. Standard deviations of sensor noises.**

| Standard deviation | Magnitude | Unit |
|---|---|---|
| $\sigma_{V_{TAS}}$ | 1 | m/s |
| $\sigma_x, \sigma_y, \sigma_h$ | 0.1 | m |
| $\sigma_\alpha, \sigma_\beta$ | $0.1\pi/180$ | rad |
| $\sigma_\phi, \sigma_\theta, \sigma_\psi$ | $0.01\pi/180$ | rad |
| $\sigma_{a_x}, \sigma_{a_y}, \sigma_{a_z}$ | 0.01 | m/s$^2$ |
| $\sigma_p, \sigma_q, \sigma_r$ | $0.01\pi/180$ | rad/s |
| $\sigma_{\delta_e}, \sigma_{\delta_a}, \sigma_{\delta_r}$ | $0.01\pi/180$ | rad |
| $\sigma_{\delta_t}$ | 0.01 | - |

Control laws are designed according to state feedbacks, and state information is acquired via sensor measurements. Noises are inevitable in measurements and control system performance is seriously affected by sensor noises. Therefore, sensor noises should be considered. In this section, sensor noises are assumed to be zero means and Gaussian distributed. Table 4 shows the standard deviations of sensor noises. Where: $\sigma_{V_{TAS}}$ represents standard deviation of pitot tube sensor, $\sigma_\alpha$, $\sigma_\beta$ represent standard deviations of airflow angle sensors, $\sigma_x, \sigma_y, \sigma_h, \sigma_\phi, \sigma_\theta, \sigma_\psi, \sigma_{a_x}, \sigma_{a_y}, \sigma_{a_z}, \sigma_p, \sigma_q, \sigma_r$ represent standard deviations of integrated navigation system sensors, $\sigma_{\delta_e}, \sigma_{\delta_a}, \sigma_{\delta_r}$ represent standard deviations of control surface deflection measurement sensors, and $\sigma_{\delta_t}$ denotes standard deviation of a throttle stick measurement sensor.

### A. CONTROL LOOPS SIMULATIONS

In real flight, the quantified structural damage induced uncertainties are unknown which are required to be estimated online. In order to demonstrate the estimation performance of

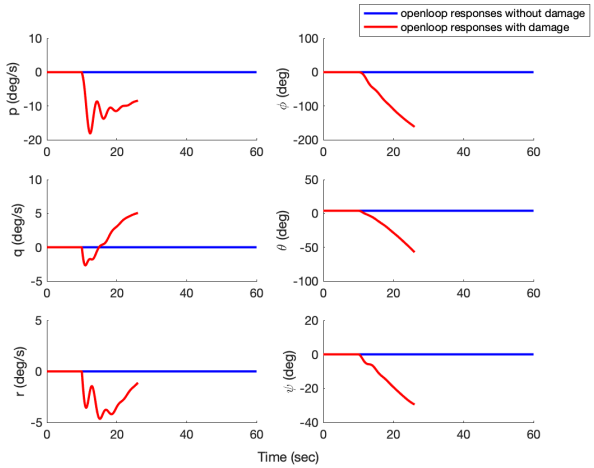


**FIGURE 3.** Rotation rates and attitude angles of open-loop responses.

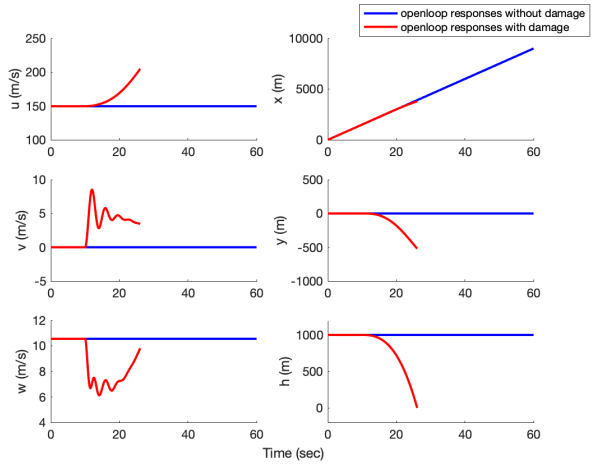


**FIGURE 4.** Velocities and positions of open-loop responses.

the control methods, the quantified structural damage induced uncertainties are injected to the model with known values. Since damage tends to reduce the energy of an aircraft, the quantified structural damage induced uncertainties are set as negative values as:

$$\triangle_{pqr} = \begin{bmatrix} \triangle_{\dot{p}} \\ \triangle_{\dot{q}} \\ \triangle_{\dot{r}} \end{bmatrix} = \begin{bmatrix} -5 \\ -5 \\ -5 \end{bmatrix} \tag{64}$$

It is injected into the simulation model since 10 *sec*, and the uint is $deg/s$.

### 1) OPEN-LOOP RESPONSES

Fig.3 shows the rotation rate and attitude angle information, and Fig.4 shows position and velocity information of open-loop responses. The blue line denotes open-loop responses of an aircraft without damage, and the red line denotes open-loop responses of an aircraft with damage. The blue line shows that the aircraft maintains stable level flight. The red line shows that the aircraft falls and breaks at 26 *sec* with a velocity at 205 $m/s$.

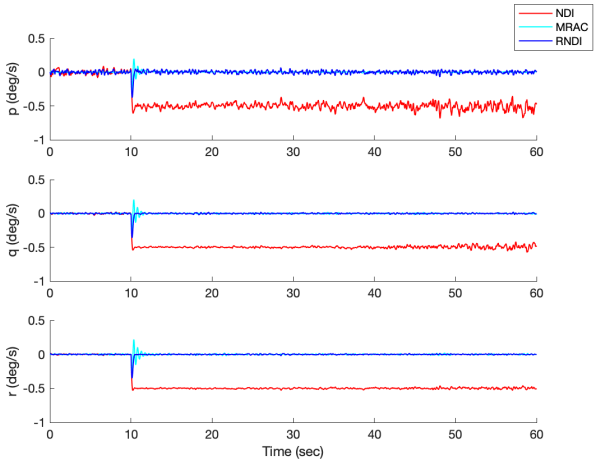


**FIGURE 5.** Rotation rates of the rotation rate control loop.

### 2) ROTATION RATE CONTROL LOOP

The control loops are divided according to the time-scale separation principle. The rotation rate control loop is inner-loop of an attitude control loop since dynamics of rotation rates are much faster than attitudes. Rotation rates usually vary quickly that a pilot cannot manually complete control objectives, therefore, the aim of an inner-loop design is to auto-stabilize an aircraft when suffering unexpectable disturbances such as damage.

Fig.5 shows rotation rate information of the rotation control loop. The red, cyan, and blue lines denote rotation rate information of damaged aircraft controlled via NDI, MRAC, and RNDI control methods respectively. Fig.6 shows quantified structural damaged induced uncertainty estimations of the rotation control loop. The red, cyan, and blue lines denote injected uncertainties, uncertainty estimations of MRAC, and uncertainty estimations of RNDI respectively.

Fig.5 demonstrates that rotation rates controlled via NDI cannot be retained after structural damage occurred at 10 *sec*, while MRAC and RNDI control methods are able to auto-stabilize a damaged aircraft. The MRAC control method appears decaying oscillations after damage occurred, whereas the RNDI control method stabilizes an aircraft in a mild way. The RNDI control method also possesses better uncertainty estimation performance than the MRAC control method as shown in Fig.6.

### 3) ATTITUDE CONTROL LOOP

An attitude control loop is relatively slow, which means that pilot is able to manually complete control objectives. While autopilot is able to precisely achieve control objectives in a short time, therefore, reducing the burden on a pilot.

Fig.7 shows rotation rates and attitude angles of the attitude control loop. The red, cyan, and blue lines denote rotation rates and attitude angles of a structurally damaged aircraft controlled via NDI, MRAC, and RNDI control methods respectively. Fig.7 demonstrates that attitude angles controlled via NDI control method cannot be retained after

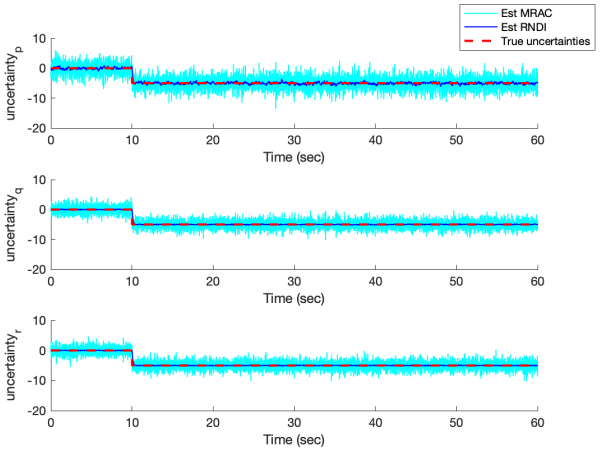


**FIGURE 6.** Uncertainty estimations of the rotation rate control loop.

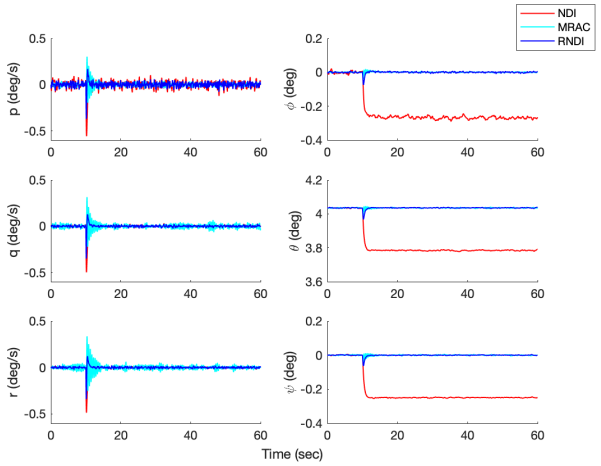


**FIGURE 7.** Rotation rates and attitude angles of the attitude control loop.

damage occurred at 10 *sec*, while MRAC and RNDI control methods are able to auto-stabilize the damaged aircraft. The MRAC control method suffers decaying oscillations in rotation rates after damage occurred, whereas the RNDI control method is able to stabilize a damaged aircraft in a mild way. For the MRAC control method, attitude angles also appear slight decaying oscillations since the oscillations appeared in the rotation rate control loop.

### *B. A STRUCTURALLY DAMAGED AIRCRAFT INSTANCE*

In order to demonstrate the effectiveness of the proposed RNDI control law in real applications, parameter changes are validated in this subsection rather than injecting known quantified model uncertainties to the model. Table 5 shows assumptive parameter changes caused by structural damage.

Fig.8 shows rotation rates and attitude angles of a structurally damaged aircraft controlled via the NDI, MRAC, and RNDI control laws respectively. Fig.9 shows structural damage induced uncertainty estimations of the MRAC and RNDI control methods. Fig.10 shows the control surface deflections of the structurally damaged aircraft.

**TABLE 5.** Parameter changes caused by structural damage.

| Parameters | Damaged parameters | Unit |
|---|---|---|
| $b_{ref}$ | $0.8 * b_{ref}$ | $m$ |
| $c_{ref}$ | $0.8 * c_{ref}$ | $m$ |
| $x_{ref}$ | $0.8 * x_{ref}$ | $m$ |
| $z_{ref}$ | $0.8 * z_{ref}$ | $m$ |
| $S_{ref}$ | $0.8 * S_{ref}$ | $m^2$ |
| $mass$ | $0.8 * mass$ | $kg$ |
| $I_b$ | $0.8 * I_b$ | $kg \cdot m^2$ |
| $C_D$ | $1.2 * C_D$ | – |
| $C_Y$ | $1.2 * C_Y$ | – |
| $C_L$ | $0.8 * C_L$ | – |
| $C_l$ | $1.2 * C_l$ | – |
| $C_m$ | $0.8 * C_m$ | – |
| $C_n$ | $1.2 * C_n$ | – |

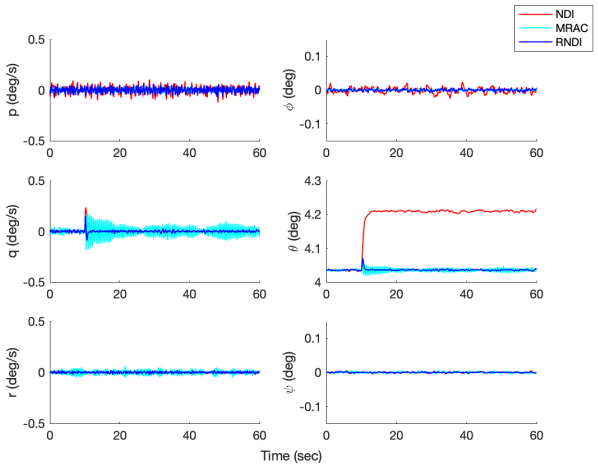


**FIGURE 8.** States of a structurally damaged aircraft.

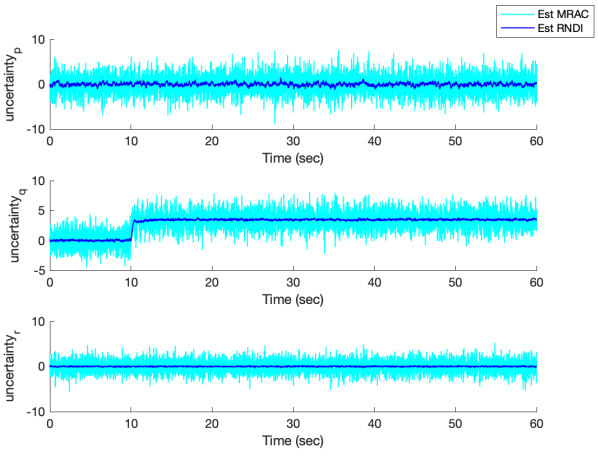


**FIGURE 9.** Uncertainty estimations of a structurally damaged aircraft.

Fig.9 shows that parameter changes induce relative large uncertainty in the $q$ channel, while relative small uncertainties in the $p$ and $r$ channels. NDI control laws do not possess uncertainty compensation mechanisms, a pitch angle $\theta$ cannot be retained due to the structural damage induced uncertainty in the $q$ channel is not compensated. Whereas,

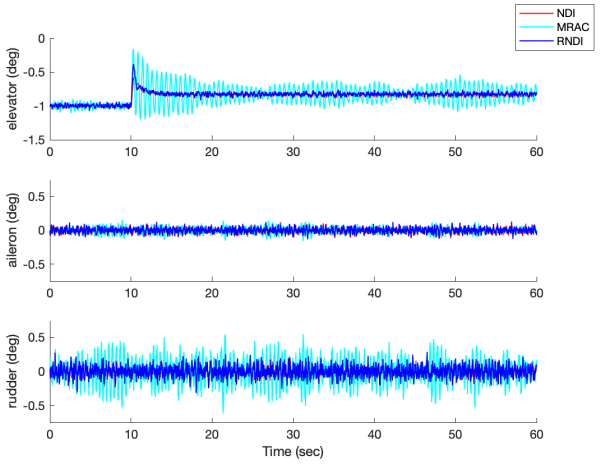


**FIGURE 10.** Control surface deflections of a structurally damaged aircraft.

the MRAC and RNDI control methods do uncertainty compensation according to the estimation results.

Dynamic responses of an aircraft are directly relevant to control surface deflections, and control surface deflections are relevant to uncertainty estimation results. From a steady view, elevators do slight deflections after damage occurred, which compensates the structural damage induced uncertainty in the $q$ channel, and ailerons and rudders do not deflect apparently due to the uncertainty estimations in the $p$ and $r$ channels are nearly zeros. From a dynamic view, oscillations of the MRAC control method are more violent than the RNDI control method due to the uncertainty estimations of the MRAC control method are more noisy, and the oscillations of the elevators and rudders cause the oscillations of the rotation rates and attitude angles.

Noisy uncertainty estimations produce the oscillations of the elevators and rudders. Compared to the MRAC control method, the control surface deflections of the RNDI control method are more mild since the uncertainty estimations of the RNDI control method are less noisy. Beyond, Fig.10 also shows that control surface responses of the NDI control method are similar to the RNDI control method, but elevator deflections of the RNDI control method are bigger than the NDI control method in 1 *sec* after damage occurred. Since the differences in the elevator deflections, the RNDI control method is able to retain the pitch angle $\theta$ and possesses smaller variation in the rotation rate $q$ after damage occurred.

### C. RESULT ANALYSIS

Structural damage induces extensive parameter changes which are unpredictable. A controller design is based on an aircraft model, mismatches between an offline model and a real aircraft lead to control performance degradation. Conventional NDI controllers are designed based on offline model, therefore it is not robust to the structural damage.

In order to overcome the mismatch problem after structural damage occurred, an online controller reconfiguration strategy is adopted in this article. The core of an online controller reconfiguration strategy is damage induced uncertainty estimations, which delivers a new model description to a controller. Afterwards, the controller reconfigures its structures according to the estimations. The proposed RNDI control method estimates quantified structural damage induced model uncertainties via using a NDO, while the MRAC control method merely differentiates sensor measurements with respect to a sample time.

**TABLE 6.** RMSEs of uncertainty estimations for the rotation rate control loop.

| Channel | MRAC | RNDI |
|---|---|---|
| $\triangle_{\dot{p}}$ | 0.0357 | 0.0065 |
| $\triangle_{\dot{q}}$ | 0.0250 | 0.0035 |
| $\triangle_{\dot{r}}$ | 0.0246 | 0.0034 |

**TABLE 7.** STDs of uncertainty estimations for the damaged aircraft.

| Channel | MRAC | RNDI |
|---|---|---|
| $\triangle_{\dot{p}}$ | 0.0370 | 0.0060 |
| $\triangle_{\dot{q}}$ | 0.0254 | 0.0035 |
| $\triangle_{\dot{r}}$ | 0.0247 | 0.0018 |

As stated in section III, structural damage induces parameter changes can be quantified as additive uncertainties in angular accelerations. In the rotation rate control loop simulation, additive uncertainties are injected to the model and the values are known, hence root mean square errors (RMSE) can be utilized to evaluate its estimation performance. While in the structurally damaged aircraft simulation, additive uncertainty values are unknown, and RMSEs cannot be exploited to evaluate the estimation performance. Instead of a RMSE, standard deviations (STD) of the estimation results after controller reconfiguration completed are used to evaluate the estimation performance.

Table 6 shows the uncertainty estimation RMSEs of the RNDI and MRAC control methods for the rotation rate control loop. Table 7 shows uncertainty estimation STDs of the RNDI and MRAC control methods for the damaged aircraft. Both RMSE and STD indices show that the RNDI control method possesses a higher order estimation accuracy than the MRAC control method. Sensor noises are inevitable, and the differential operation of the MRAC control method amplifies the sensor noises. Whereas, a NDO is able to obtain high quality uncertainty estimations without a differential operation. High quality uncertainty estimations mean that a NDO delivers a more precise model description to the reconfigurable controller which is crucial to control performance. Fig.8 - Fig.10 show that noisy uncertainty estimations of the MRAC control method lead to oscillations in control surfaces and states. Whereas, oscillations do not appear in the proposed RNDI control method, where the superiority lies in.

## V. CONCLUSION

For model-based flight controller design, model uncertainties and sensor noises deteriorate control performance significantly. Structural damage induces extensive parameter

changes of an aircraft, this article quantifies the extensive parameter changes as model uncertainties in accelerations and angular accelerations. The proposed RNDI controller is composed of a NDO and a modified NDI controller. The NDO is explored to estimate the uncertainties, and the estimations are fed to the modified NDI controller. Simulation results demonstrate that the proposed RNDI control law possesses a satisfactory control performance compared with NDI and MRAC control laws.

NDI is a nonlinear control technique which need not schedule gains in a flight envelope. But it is not robust to model uncertainties, control performance degrades significantly when model uncertainties exist. Based on the reconfiguration mechanism proposed in this article, the MRAC control method is robust to model uncertainties. But due to the angular accelerations are acquired via differentiating gyroscope measurements, which causes noise amplifications in feedbacks. The noise amplifications lead to oscillations, which are undesired in control system.

The proposed RNDI control law not only need not schedule gains in a flight envelope, but also is robust to model uncertainties. The quantified model uncertainties in angular accelerations are estimated via a NDO. The NDO synthesizes control inputs and sensor measurements, which need not differentiate gyroscope measurements with respect to sample time. Therefore, noise amplifications and oscillations are not appeared in the RNDI control method. But a NDO increases computational complexity, which leads to the RNDI control method possesses slowest running speed compared with NDI and MRAC control methods. While, as the growth of calculate ability of microprocessors, running a RNDI control law in real time is not a problem at all.

## ACKNOWLEDGMENT

The authors would like to sincerely thank the anonymous reviewers and the editors who provided appropriate suggestions and detailed corrections, and have made the article much more readable.

## REFERENCES

[1] A. Fekih and P. Pilla, "A passive fault tolerant control strategy for the uncertain MIMO aircraft model F-18," in *Proc. Southeastern Symp. Syst. Theory*, Macon, GA, USA, Mar. 2007, pp. 320–325.
[2] X. Li and H. H. T. Liu, "A passive fault tolerant flight control for maximum allowable vertical tail damaged aircraft," *J. Dyn. Syst., Meas., Control*, vol. 134, no. 3, May 2012.
[3] J. Zhao, B. Jiang, P. Shi, and Z. He, "Fault tolerant control for damaged aircraft based on sliding mode control scheme," *Int. J. Innov. Comput., Inf. Control*, vol. 10, no. 1, pp. 293–302, 2014.
[4] X. Yu and Y. Zhang, "Design of passive fault-tolerant flight controller against actuator failures," *Chin. J. Aeronaut.*, vol. 28, no. 1, pp. 180–190, Feb. 2015.
[5] A. Nasiri, S. K. Nguang, A. Swain, and D. Almakhles, "Passive actuator fault tolerant control for a class of MIMO nonlinear systems with uncertainties," *Int. J. Control*, vol. 92, no. 3, pp. 693–704, Mar. 2019.
[6] Z. Hou, P. Lu, and Z. Tu, "Nonsingular terminal sliding mode control for a quadrotor UAV with a total rotor failure," *Aerosp. Sci. Technol.*, vol. 98, p. 105716, 2020.
[7] A. Fekih, "Fault diagnosis and fault tolerant control design for aerospace systems: A bibliographical review," in *Proc. Amer. Control Conf.*, Portland, OR, USA, Jun. 2014, pp. 1286–1291.
[8] J. Cieslak, D. Henry, A. Zolghadri, and P. Goupil, "Development of an active fault-tolerant flight control strategy," *J. Guid., Control, Dyn.*, vol. 31, no. 1, pp. 135–147, Jan. 2008.
[9] Y. Zhang and J. Jiang, "Bibliographical review on reconfigurable fault-tolerant control systems," *Annu. Rev. Control*, vol. 32, no. 2, pp. 229–252, Dec. 2008.
[10] C. Edwards, T. Lombaerts, and H. Smaili, *Fault Tolerant Flight Control*. Cham, Switzerland: Springer, 2010.
[11] R. Hallouzi and M. Verhaegen, "Fault-tolerant subspace predictive control applied to a boeing 747 model," *J. Guid., Control, Dyn.*, vol. 31, no. 4, pp. 873–883, Jul. 2008.
[12] D. Joosten, T. Boom, and T. Lombaerts, "Computationally efficient use of MPC and dynamic inversion for reconfigurable flight control," in *Proc. AIAA Guid., Navigat. Control Conf. Exhib.*, Honolulu, HI, USA, Aug. 2008, p. 7431.
[13] T. J. J. Lombaerts, H. O. Huisman, Q. P. Chu, J. A. Mulder, and D. A. Joosten, "Nonlinear reconfiguring flight control based on online physical model identification," *J. Guid., Control, Dyn.*, vol. 32, no. 3, pp. 727–748, May 2009.
[14] P. Castaldi and N. Mimmo, "Aircraft nonlinear AFTC based on geometric approach and singular perturbations in case of actuator and sensor faults," *IFAC Proc. Volumes*, vol. 46, no. 19, pp. 30–35, 2013.
[15] Y. Jiang, S. Yin, and O. Kaynak, "Data-driven monitoring and safety control of industrial cyber-physical systems: Basics and beyond," *IEEE Access*, vol. 6, pp. 47374–47384, 2018.
[16] E. Kamal, A. Aitouche, R. Ghorbani, and M. Bayart, "Robust fuzzy fault-tolerant control of wind energy conversion systems subject to sensor faults," *IEEE Trans. Sustain. Energy*, vol. 3, no. 2, pp. 231–241, Apr. 2012.
[17] B. Jiang, Z. Gao, P. Shi, and Y. Xu, "Adaptive fault-tolerant tracking control of near-space vehicle using Takagi–Sugeno fuzzy models," *IEEE Trans. Fuzzy Syst.*, vol. 18, no. 5, pp. 1000–1007, Oct. 2010.
[18] C. Hu, X. Zhou, B. Sun, W. Liu, and Q. Zong, "Nussbaum-based fuzzy adaptive nonlinear fault-tolerant control for hypersonic vehicles with diverse actuator faults," *Aerosp. Sci. Technol.*, vol. 71, pp. 432–440, Dec. 2017.
[19] D.-H. Shin and Y. Kim, "Reconfigurable flight control system design using adaptive neural networks," *IEEE Trans. Control Syst. Technol.*, vol. 12, no. 1, pp. 87–100, Jan. 2004.
[20] C. Y. Huang and R. F. Stengel, "Restructurable control using proportional-integral implicit model following," *J. Guid., Control, Dyn.*, vol. 13, no. 2, pp. 303–309, Mar. 1990.
[21] M. Bodson and J. E. Groszkiewicz, "Multivariable adaptive algorithms for reconfigurable flight control," *IEEE Trans. Control Syst. Technol.*, vol. 5, no. 2, pp. 217–229, Mar. 1997.
[22] J. D. Boskovic and R. K. Mehra, "Intelligent adaptive control of a tailless advanced fighter aircraft under wing damage," *J. Guid., Control, Dyn.*, vol. 23, no. 5, pp. 876–884, Sep. 2000.
[23] E. Lavretsky, "Combined/Composite model reference adaptive control," *IEEE Trans. Autom. Control*, vol. 54, no. 11, pp. 2692–2697, Nov. 2009.
[24] N. Nguyen, K. Krishnakumar, J. Kaneshige, and P. Nespeca, "Dynamics and adaptive control for stability recovery of damaged asymmetric aircraft," in *Proc. AIAA Guid., Navigat., Control Conf. Exhib.*, Keystone, CO, USA, Aug. 2006, p. 6049.
[25] V. V. Patel, C. Cao, N. Hovakimyan, K. A. Wise, and E. Lavretsky, "L1 adaptive controller for tailless unstable aircraft," in *Proc. Amer. Control Conf.*, New York, NY, USA, Jul. 2007, pp. 5272–5277.
[26] D. Jourdan, M. Piedmonte, V. Gavrilets, D. Vos, and J. McCormick, "Enhancing UAV survivability through damage tolerant control," in *Proc. AIAA Guid., Navigat., Control Conf.*, Toronto, ON, USA, Aug. 2010, p. 7548.
[27] Q. He, W. Zhang, P. Lu, and J. Liu, "Performance comparison of representative model-based fault reconstruction algorithms for aircraft sensor fault detection and diagnosis," *Aerosp. Sci. Technol.*, vol. 98, Mar. 2020, Art. no. 105649.
[28] P. Lu, E.-J. van Kampen, C. de Visser, and Q. Chu, "Aircraft fault-tolerant trajectory control using incremental nonlinear dynamic inversion," *Control Eng. Pract.*, vol. 57, pp. 126–141, Dec. 2016.
[29] W.-H. Chen, D. J. Ballance, P. J. Gawthrop, and J. O'Reilly, "A nonlinear disturbance observer for robotic manipulators," *IEEE Trans. Ind. Electron.*, vol. 47, no. 4, pp. 932–938, Dec. 2000.

**QIZHI HE** was born in September 1992. He received the B.Eng. degree from Northwestern Polytechnical University, in 2013, and the M.A.Sc. degree (Hons.) from the University of Leicester, in 2015. He is currently pursuing the Ph.D. degree in control science and engineering with Northwestern Polytechnical University. He has published more than ten articles in relevant fields. His research interests include fault tolerant flight control and multisensor information fusion theory.

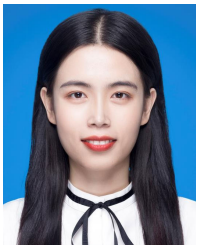

**YI TAN** was born in August 1995. She received the bachelor's degree in mechanics from Northwestern Polytechnical University, in 2018, where she is currently pursuing the master's degree in control science and engineering. Her research interests include flight control and active flow control technology, including active jet method and plasma flow control method.

**XIAOXIONG LIU** received the B.Eng. degree in mechatronic engineering and the M.Eng. and Ph.D. degrees in navigation, guidance, and control from Northwestern Polytechnical University, Xi'an, China, in 1998, 2004, and 2006, respectively. He is currently an Associate Professor with Northwestern Polytechnical University. He has presided two projects of the Aviation Fund and ten other projects. He has more than 50 academic articles have been published in journals and international conferences. His current research interests include aircraft flight control technology, UAV autonomous control technology, guidance and navigation technology, fault diagnosis, and fault tolerance flight control technology.

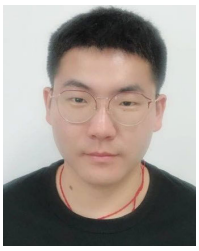

**QIANLEI JIA** received the B.Eng. degree in automation from Northwestern Polytechnical University, Xi'an, China, in 2015, where he is currently pursuing the Ph.D. degree in control science and engineering. His research interests include aircraft control, air combat decision-making, and fault detection.

**JINGLONG LIU** was born in March 1988. He received the M.A.Sc. degree from Xi'an Jiaotong University, in 2013, and the Ph.D. degree in control science and engineering from Northwest Polytechnic University, in 2019. He is currently with the Shanghai Institute of Aerospace System Engineering. He has also published nearly ten articles and patents in academic conferences and journals. His current research interests include gust load alleviation technology, flight control technology, multicontrol-effectors plane control allocation technology, space robotic manipulator control technology, and space docking mechanism control technology.